

Analysis and study of the influence of the geometrical parameters of mini unmanned quad-rotor helicopters to optimise energy saving

I. Penkov¹ and D. Aleksandrov²

¹School of Engineering, Department of Mechanical and Industrial Engineering,
Tallinn University of Technology, Estonia
E-mail: igor.penkov@ttu.ee, Phone: +3725169922

²PLM Group, Estonia

ABSTRACT

The article discusses lift force generated by mini UAVs (Unmanned Aerial Vehicles). CFD (Computational Fluid Dynamics) simulations were made on the base of a 3D scanned propeller model. Influence of some geometrical parameters of propeller (like velocity or pitch) and quadcopter (like gap) on lifting force was considered. Different propeller pitches were used and pitch influence on propeller lift force was analysed. Normally, lifting force will increase with the increasing of propeller pitch but for different rotation velocities, this increasing is different and in all cases, it can be approximated by a linear relationship. To obtain dependency functions, an equation for calculation of lift force given took into account the correction coefficients. This equation gave reliable results at pitch values equal to 0.3 – 0.7 of the propeller diameter and at rotation velocities of 2000 min⁻¹ – 8000 min⁻¹.

Lift force dependency from distance between rotors was also considered. Simulations and experiments showed that the lifting force of a quadcopter increased about 15% on gap distances from 5 mm to 35 mm. From a distance of 70 mm, the lifting force will decrease about 2% and then will stabilise. At increasing of distance between propellers from 5 mm until 25 mm, the power consumption decreased 8% - 10% and after the gap distance equal to 40 mm, it will be stable and minimal. It can be asserted that quadcopters have different optimal distances between the propellers at different rotation speeds to generate the same force. Equations for calculation of optimal gap distances for different multicopters were derived and calculation results are presented in graphs and tables.

Keywords: UAV, CFD Simulation, Quadcopter, Lift Force, Rotor, Gap, Energy Saving.

INTRODUCTION

In the last decades, many autonomous and teleoperated vehicles in the applications of robotics have been developed, including wheeled or tracked and legged vehicles. However, in many cases, ground vehicles have significant inherent limitations to access desired locations due to the characteristics of the terrain and the presence of obstacles. In these cases, aerial vehicles are the natural way to approach the objective to obtain information or even to perform necessary actions such as the deployment of instrumentation [1]. Unmanned aerial vehicles are widely used in various civil [2, 3] and military [4] applications, for example for traffic monitoring [5, 6], navigation [7, 8] and aerial mapping. UAVs are used for agriculture [9, 10] needs, press, television,

cinematography [11, 12], marine application, pollution detection and other fields. UAVs are capable of carrying out work under conditions where the surrounding environment is dangerous or not accessible to humans. They can carry out many military applications such as border patrol monitoring [13] and drug smugglers detection, uninhabited combat aerial vehicles and radar saturation roles. UAVs have generated great interest in industrial and academic areas [14-16] due to small size [17-19], unique flight capacities [20-22], outstanding maneuverability and low cost. A lot of researches related to stability and controllability are being conducted [23-26]. Mathematical calculation methods, basis of screw theory [27], analysis of joining between components [28] and optimisation of kinematic parameters [29] are also usually used for the development of UAVs.

One very important part in analysing UAVs is rotors energy saving and increasing the system capacity. Many different parameters like mass, design, environment and other influence on energy consumption [30-32]. The work by [33] tried to save system energy by chattering reduction during mini UAV control. Work by [34, 35] considered thrust optimisation in rotors with two and three propellers. The main purposes of this research are to consider the influence of rotor pitch and gap between rotors on lift force and power consumption of a quadcopter. Analysis will be done with the help of CFD simulations and laboratory tests. Normally, the increase in propeller pitch causes increase in lifting force magnitude but it is interesting to know the influence of different velocities. Relationship between lifting force produced by rotors and quadcopter mass gives information about system efficiency and it is beneficial to know the optimal design parameters in a quadcopter.

METHODS AND MATERIALS

CFD Modelling

Lifting force generated by propeller was carried out owing to an air flow created near the propeller and directed down (Figure 1). The simulating models (Figure 2 (a)) were created on the base of real propellers (DF-1050CR from Draganfly Innovations, airfoil type similar to NACA6409) with diameter of 254 mm and pitch of 127 mm as well as a propeller with diameter of 203.2 mm and pitch of 101.6 mm, scanned with the help of a 3D scanner. The scanned models were imported in SolidWorks Flow Simulation as point cloud data [36]. Then, working models were created and lifting force of propellers was determined at different rotation speeds.

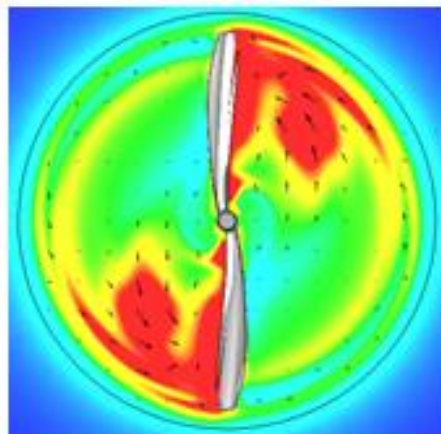


Figure 1. Air stream near the propeller.

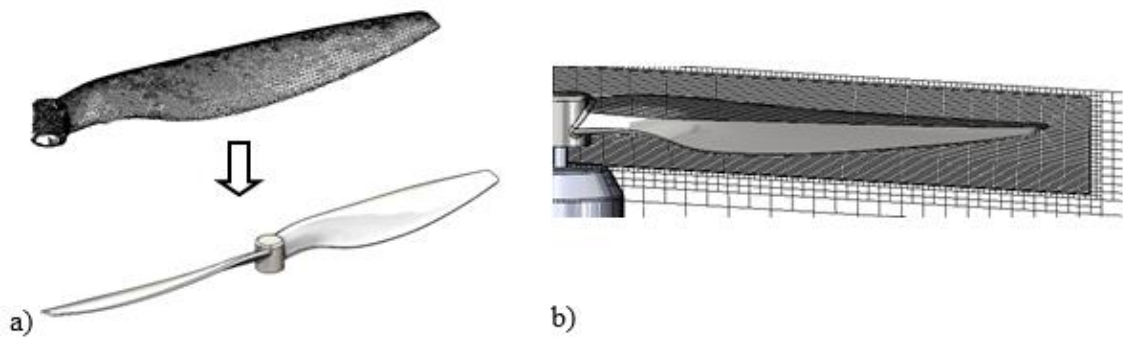


Figure 2. Models for CFD simulation for 254 mm propeller (a) 3D scanned data; (b) FVM mesh.

CFD simulations were made using external computational domain with a local rotating region. The environment was filled by air with a density of 1.2 kg/m^3 . Normal environmental conditions with pressure 101325 Pa and temperature 293.2 K were used. Temperature change effects were not taken into account. Meshing was done by manual mesh control using planes and mesh refinement around the propeller's curved surfaces (Figure 2(b)). Mesh refinement reduced the number of partial cells (cells that were partly solid and partly fluid). All the simulations were made in steady-state mode until convergence of the lifting force was less than 0.02 N (around 0.3% of the whole amount of the lifting force). In Figure 3, streamlines and vectors show air velocity and flow direction. Colours show pressure difference near the rotating propeller. Pressure difference between the top and bottom surfaces of the propeller generated the lifting force. Edges of the rotating propeller created a turbulent area, where the flow went upwards and this stream partially compensated lower pressure region on top and the lifting force decreased.

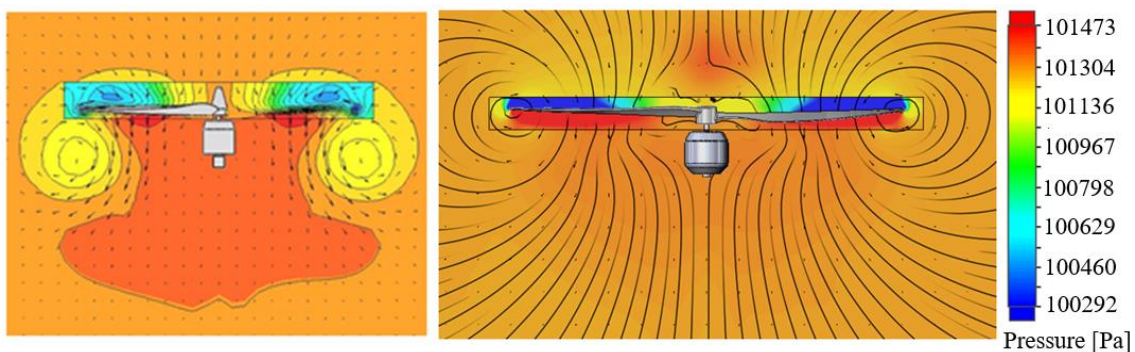


Figure 3. Pressure distribution near the propeller.

Experiments Study

In the experiments, a brushless motor Robbie 2827-34 with propellers 254 x 127 mm and 203.2 x 101.6 mm was used. For motor control, a brushless motor controller (ESC) BL-CTRL 1.2 from the Mikrokopter Company was used, operated through RS232 port directly from PC (using UM232R USB Serial UART Development Module by FTDI Company). For control, freeware software KopterTool V1_78B from a brushless motor controller developer was used. To determine motor power consumption, a bypass resistor was used. Experiments were made by help of a testing device shown in Figure 4. Heavy

base was fixed with a strain gauge sensor PS-08844244 to a motor with a propeller fixed to it. Propeller rotation speed was measured with an optical laser tachometer Omron CT6. Altogether, ten values of rotational speed were measured for each propeller size.



Figure 4. Testing device for the determination of propeller lifting force.

RESULTS AND DISCUSSION

Experiment results (Figure 5) were approximated using non-linear regression analysis software [37]. Lifting force dependency on the propeller rotation speed can be expressed as follows:

$$F = 0.486 \cdot 10^{-6} \cdot n^{1.882} \quad (1)$$

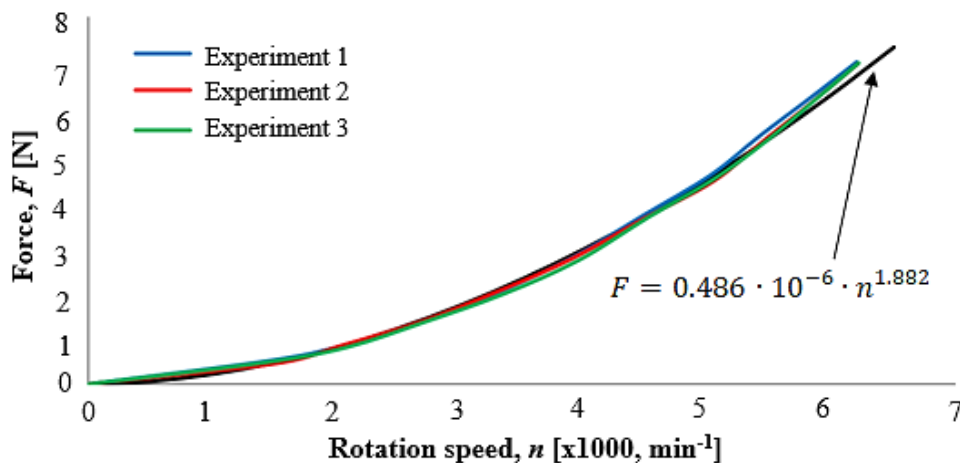


Figure 5. Data of three experiments and approximated result of the dependency of the lifting force on the rotation speed (254 mm propeller).

Power Consumption Measurement

Power consumption was measured by a bypass resistor SH-15-30A-75 with voltage 75 mV and current 15/30 A. Results of the experiments with a 254 mm propeller are shown in Figure 6. Each step on the graph corresponds to a certain propeller rotation speed and energy consumption in hovering was stable. Figure 7 shows the dependency of the lifting force on motor power consumption. Motor power consumption behaviour can be

described as linear (Figure 7), at least at working angular velocities (when rotor creates 1.0 – 7.0 N of lifting force). In the considered case, the influence of rotation speed on power consumption was also close to linear. Usually, the dependency of rotation speed on the motor energy consumption has a parabolic form, where the power consumption is proportionally lower at lower velocities than at higher.

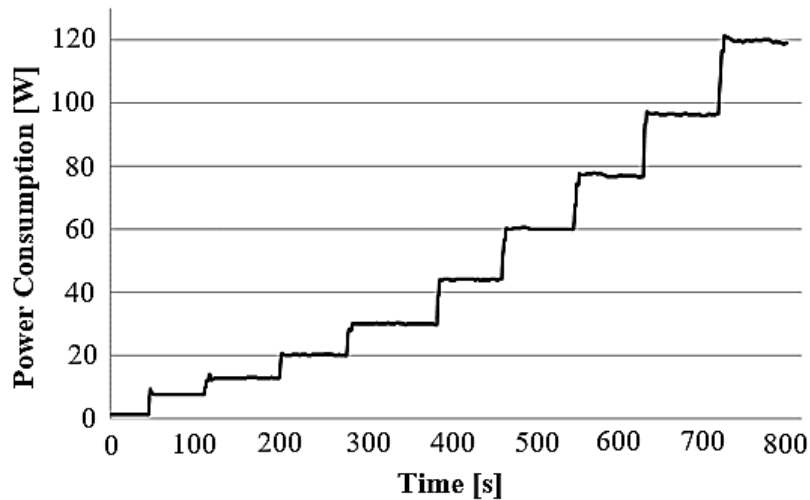


Figure 6. Motor power consumption in time.

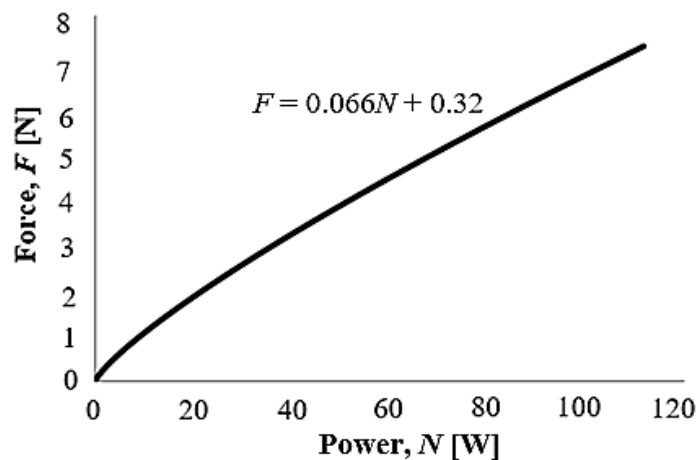


Figure 7. Dependency of the lifting force on motor power consumption.

Comparison of Simulation and Experiment Results

Figure 8 illustrates force dependency on the propeller rotation speed (Figure8 (a) compares forces produced by 254 x 127 mm propeller and Figure 8(b) shows the same data for 203.2 x 101.6 mm propeller). Experiment force graphs were made on the base of the tests data and CFD force graphs by simulations. Both methods gave approximately similar results. Maximum deflection between simulations and experiment data was about 3%. This means that the current CFD software can be used for similar analysis and comparison of propellers with different parameters.

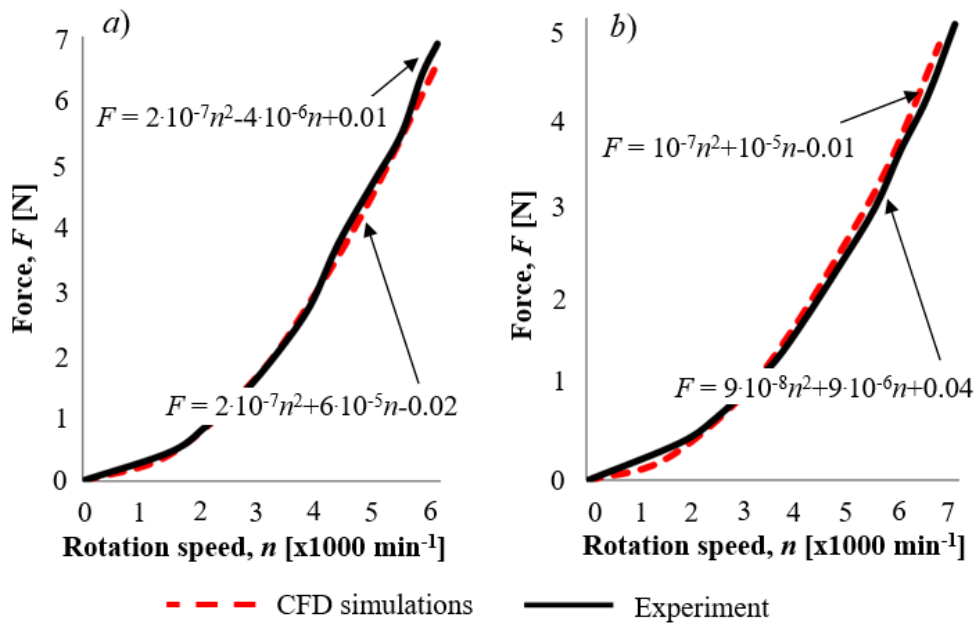


Figure 8. Dependency of the lifting force on the rotation speed; (a) 254 x 127 mm propeller; (b) 203.2 x 101.6 mm propeller.

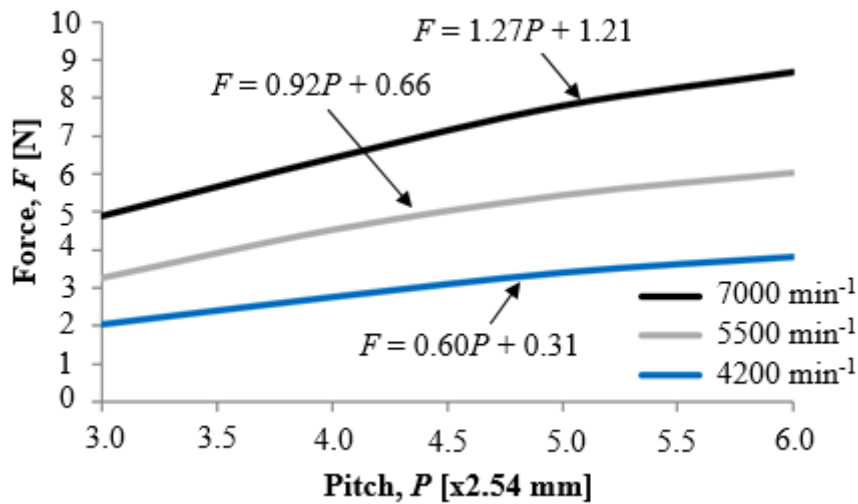


Figure 9. Dependency of the lifting force on pitch for 254 mm propeller.

Propeller Pitch Influence on Lift Force

Propellers with the same diameter can have different pitches. Let us consider pitch influence on lift load value. Theoretically, the higher the pitch, the higher the lifting force that can be produced but in reality, an increase in pitch size will generate an additional load on the motor and its combination with the propeller can be ineffective. Usually, pitch changes in the range of 0.7 – 1.3 radius of the propeller. Median value of pitch is half of a propeller’s diameter. All the other calculations have this ratio between pitch and propeller diameter. Let us consider the influence of pitch on the lifting force. Simulations compare propellers with the same diameter and rotating velocity but with different pitches. Figure 9 shows the dependence of the lifting force on the propeller pitch for different rotation speeds. All these functions can be described by linear laws with a high coefficient of determination. Simulations were made only on “working” rotation speeds

that can be used in reality (2000 – 8000 min⁻¹). Common dependency between propeller pitch and lifting force can be found by considering all three lines (Figure 9) together. Change of lift force can be presented by correction values that for example for 254 mm (10 inch) propeller can be expressed by Eq. 2. The equation takes into account both positive and negative values, depending on the pitch more or less than 127 mm (half of the propeller diameter). Adding parameter F_{C-10} to the value of lifting force (Eq. 1) can show lifting forces generated by propeller with pitches different from half of the propeller diameter. This equation is not related to the rotation speed (and therefore unrelated to the exact lifting force) and can be used only for defined velocities.

$$F_{C-10} = (P - 127) \cdot 0.037 \quad (2)$$

Simulations for the determination of the dependency of the lifting force on pitch were also made for 203.2 mm and 304.8 mm rpropellers (8 inch and 12 inch). Those dependencies were also linear and can be described by Eq. 3 (similar to Eq. 2).

$$F_{C-8} = (P - 101.6) \cdot 0.018, \quad F_{C-12} = (P - 152.4) \cdot 0.051 \quad (3)$$

Combination of Eq. 2 and 3 will result in the overall correction coefficient F_C (Eq. 4). Using the parameter F_C , it is possible to forecast how the lifting force will change if the propeller pitch will be different from half of the diameter. This formula gives reliable results at pitch values equal to 0.3 – 0.7 of the propeller diameter and at rotation velocities 2000 – 8000 min⁻¹.

$$F_C = \left(P - \frac{D}{2}\right) \cdot \left(3.27 \cdot 10^{-4} D - 4.72 \cdot 10^{-2}\right) \quad (4)$$

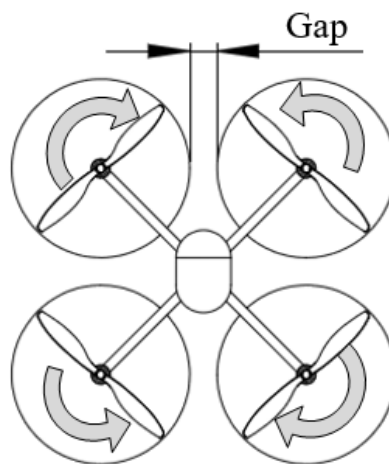


Figure 10. Simplified model of a quadrotor helicopter for CFD simulation.

Optimal Gap Between Propellers

Influence of Distance between the Propellers on the Lifting Force

The laminar and turbulent flows were created near the rotating propeller (Figures 1 and 3). When multicopter propellers were very close to each other, flows from them affected neighbouring propellers and their motor power consumption. With increasing distance between the propellers, the mass and dimensions of the helicopter increased and it is

necessary to know an optimal gap distance between the propellers. In this case, the helicopter mass will be at minimum and propellers will generate a maximum lifting force – influence of border effect was minimal. To determine optimal distances, lifting forces of four-rotor flying platforms (mini UAV) with different distances between propellers were analysed. The air out-flows from the propellers were simulated and the lifting force was determined with CFD software. Figure 10 shows simplified model of a quadrotor helicopter for CFD simulation. Helicopters with different distances between the propellers at different angular velocities were compared. To compare the obtained results with real conditions, a series of experiments were done.

Simulations

Simulations for lifting force determination and gap distance optimisation were made on the base of a simplified quadrotor helicopter model with 254 mm propellers. Separate simulations for four different rotation speeds 1500 min^{-1} , 3000 min^{-1} , 4000 min^{-1} and 5000 min^{-1} were done [35]. For each rotation speed, the distance range between the propellers changed from 5 mm to 140 mm (Figure 11). Environmental conditions used were the same as before: air density was 1.2 kg/m^3 , pressure 101325 Pa and temperature 293.2K. Results of the simulations showed that the lifting force produced by one propeller in quadrotor increased on distances from 5 mm to 35 mm (Figure 11) by about 15%. From a distance of 70 mm, the lifting force will decrease by about 2% and then will stabilise. This magnitude of lifting force was equal to the lifting force produced by one separately working propeller.

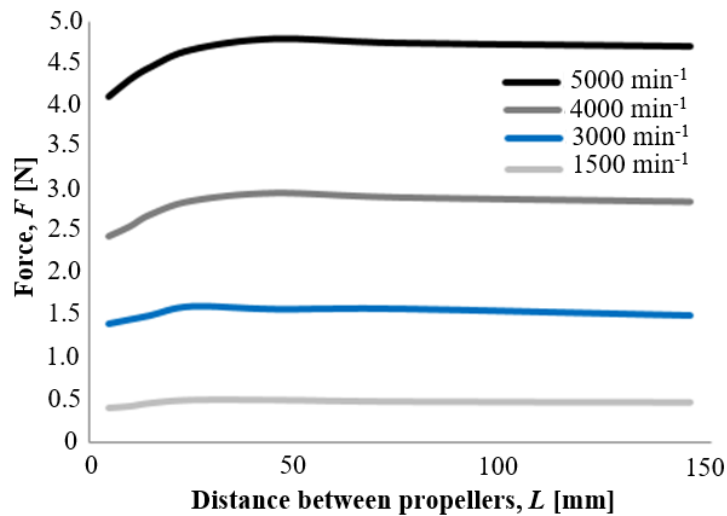


Figure 11. Dependency of the lifting force on the distance between the propellers.

Figure 12(a) shows airflow velocities and their directions of a quadrotor helicopter (front and top views) with 10 mm distance between the propellers. Velocity range was 0 – 13 m/s, darker areas near the propeller showed higher velocities. Small turbulent areas appeared near the propeller edge where air flow was twisting upwards. There was a space between the propellers where airflows were running into each other and the resulting flow moved upwards. This stream partially compensated the lifting force. Figure 12(b) illustrates airflow velocities and their directions when the distance between the propellers was 140 mm. At this distance, the influence of airflows from the propellers was insufficient. Each propeller can be considered as separately working and total lifting force

produced by quadcopter can be found as the sum of lifting forces produced by four propellers.

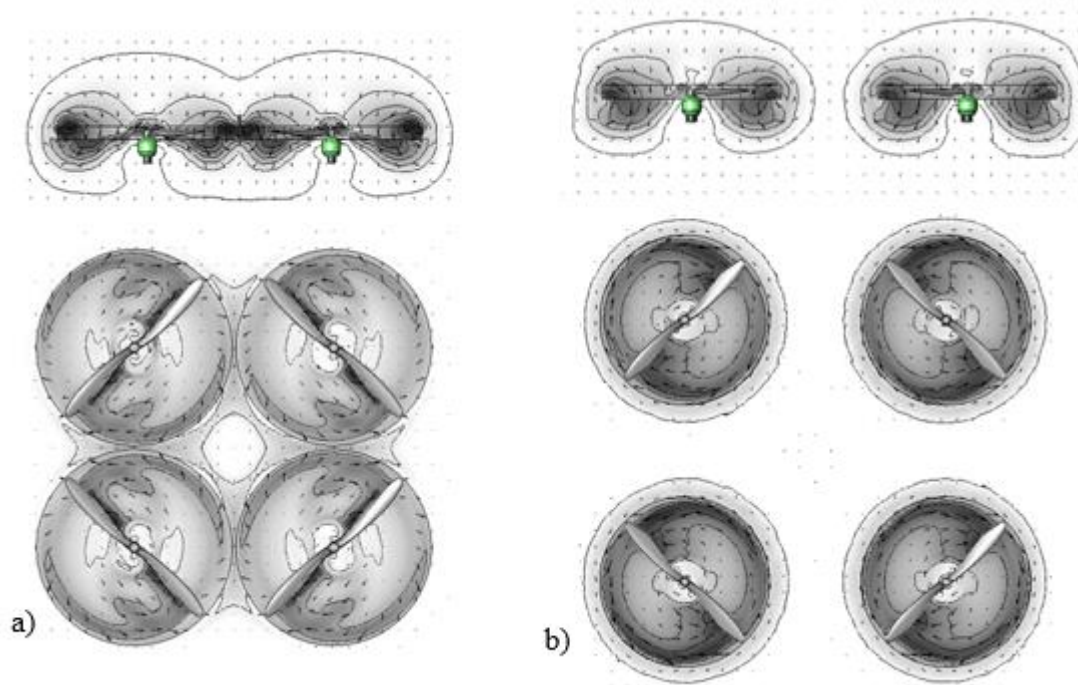


Figure 12. Air velocity distribution near the propellers.

a) distance between propellers is 10 mm, and b) distance between propellers is 140 mm

Experiments Details

A testing device was designed for experiments that allowed imitating a quadcopter with changing distance between the propellers. One of the four propellers was fixed on the force measurement device and the distance between propellers changed with steps of 10 mm.

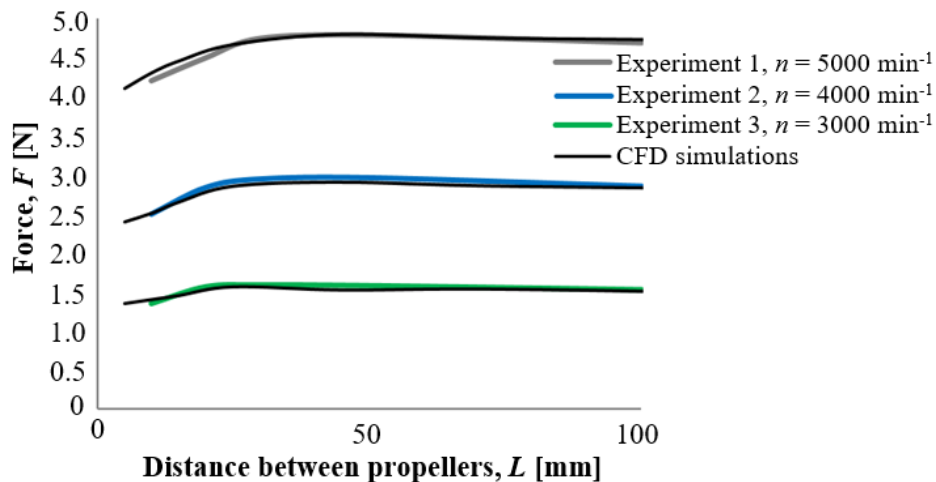


Figure 13. Dependency of the lifting force on the distance between the propellers. Comparison of experiment results with the CFD simulations.

Figure 13 illustrates the dependency of the lifting force on the distance between the propellers for different rotor angular velocities. Both experiments and CFD simulations gave approximately similar results (maximum deviation is about 3%). From Fig. 13, it can be seen that at the same angular velocity, the propeller can produce different lifting forces on different distances between the propellers. For example, at the angular velocity of 5000 min^{-1} a propeller produced 14.82% higher lifting force at distance between rotors equal to 40 mm than at the distance equal to 10 mm. By increasing the distance between propellers from 5 mm until 25 mm, the power consumption decreased 8% - 10% and after the gap distance equal to 40 mm it will be stable and minimal. Figure 14 shows the dependency of motor power consumption on the distance between the propellers for different lifting forces produced by the rotor. Difference between optimal and the highest power consumption was 9.67% (without taking into account the increasing of quadcopter mass) while the propeller created a lifting force of 5 N.

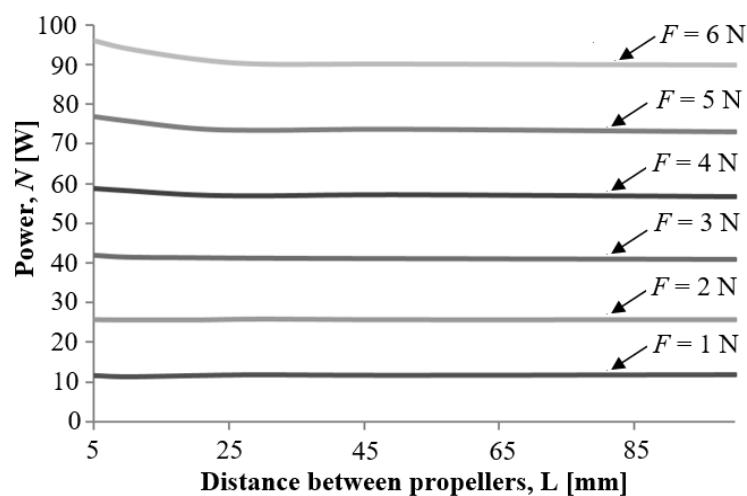


Figure 14. Dependency of motor power consumption on the distance between the propellers.

Optimal Gap Distance Determination

Optimal gap distance between the propellers is the distance when the propellers generate a maximum lifting force – air flows affect each other minimally. This distance should be considered in the hovering of a quadcopter. Helicopter mass is usually known and this fact allows easy-to-determine necessary lifting force produced by each propeller. To determine an optimal distance between propellers, it is necessary to know the energy quantity for producing a definite amount of lifting force. Since it is impossible to determine the real energy consumption by CFD software, propeller angular velocity was used as a compared parameter. To convert data, nonlinear regression analysis was made using Microsoft Excel Analysis ToolPack. Results are shown in Figure 15. Presented here are the angular velocities necessary for generating a definite amount of lifting force on a definite distance between the propellers. For example, to produce a lifting force equal to five newtons, the propeller needs to have the rotation velocity of 5698 min^{-1} at distance between propellers equal to 5 mm and a distance of 41 mm, this velocity should be only 5319 min^{-1} . For a precise determination of the optimal distance, the mass of the aerial vehicle had to be taken into account. Hereinafter was assumed that the mass per length of the UAV girder was equal to 0.25 g/mm . Thus, at the increasing of the distance between the rotors, the mass of the quadcopter also increased and a bigger lifting force was

necessary for holding an aerial vehicle immovable in air. Figure 16 shows the dependency of the propeller angular velocity on the distance between the propellers for generating 5 N of lifting force. In this case, the optimal distance was equal to 41 mm.

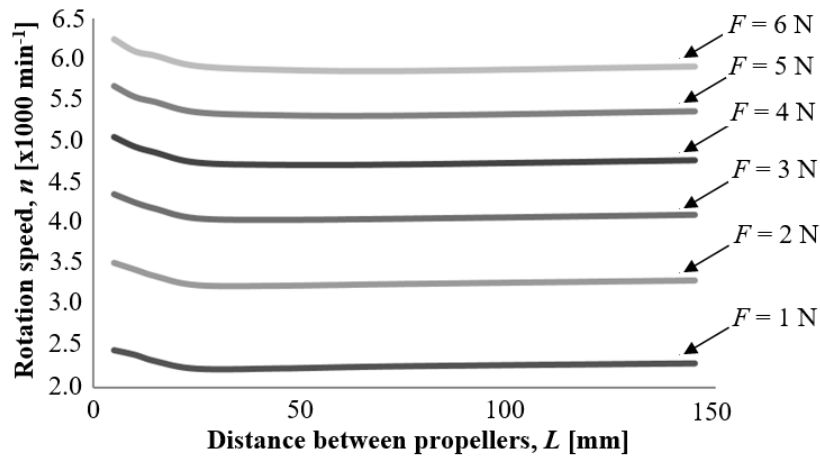


Figure 15. Dependency of the propeller rotation speed on the distance between the propellers. The propeller is producing a definite lifting force.

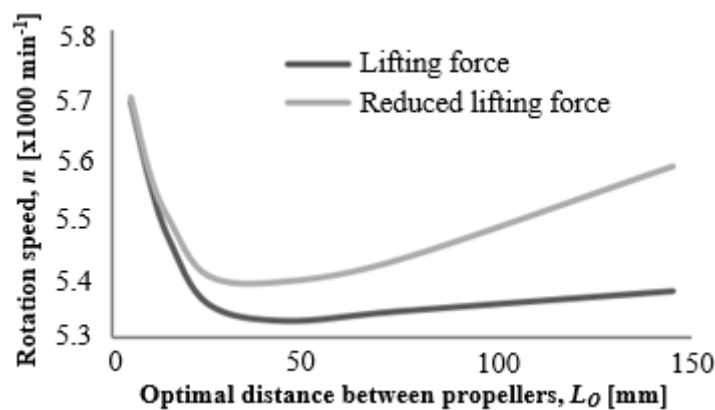


Figure 16. Optimal distance between 254 mm propellers at producing of 5 N force.

From Figure 16 it can be seen that the 254 mm quadcopters have different optimal distances between the propellers at different rotation speeds to generate the same force. The same data obtained from non-linear regression was used (Figure 15) to find optimal distances that corresponded to different lifting forces (Figure 17). Distance dependency on the lifting force for 254 mm propellers can be calculated by Eq. (5)

$$L_{O-10} = 0.55F_1^2 - 0.24F_1 + 29.75. \quad (5)$$

To create the calculation method of optimal gap distance, CFD simulations, in addition to the propeller 254 x 127 mm, were done for propellers 203.2 x 101.6 mm and 304.8 x 152.4 mm. The calculations were done on different distances between propellers and different angular velocities with the same parameters that were used for 254 mm propeller calculations. Figure 18 shows the comparison between the lifting forces produced by three different propellers at the angular velocity of 5000 min⁻¹.

Dependencies of optimal distances on the propeller diameter for different lifting forces are presented in Figure 19. It can be seen that these dependencies can be represented by similar laws for forces 2 N, 4 N, and 6 N. Common dependency can be described by Eq. 6

$$L_d = 0.15 \cdot D - 38.10 \quad (6)$$

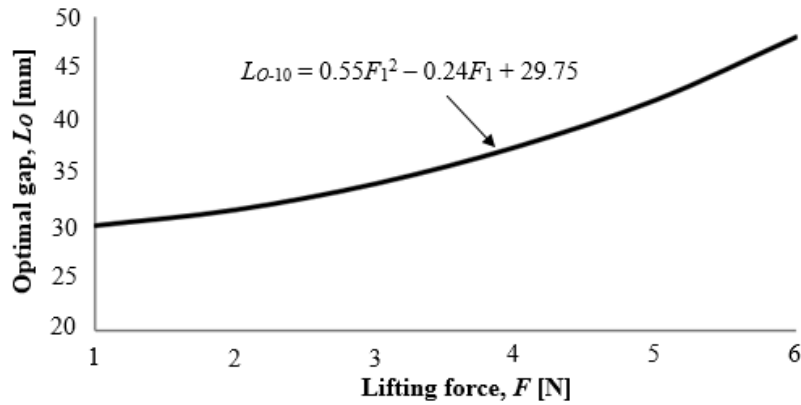


Figure 17. Optimal distances between 254 mm propellers for different lifting forces.

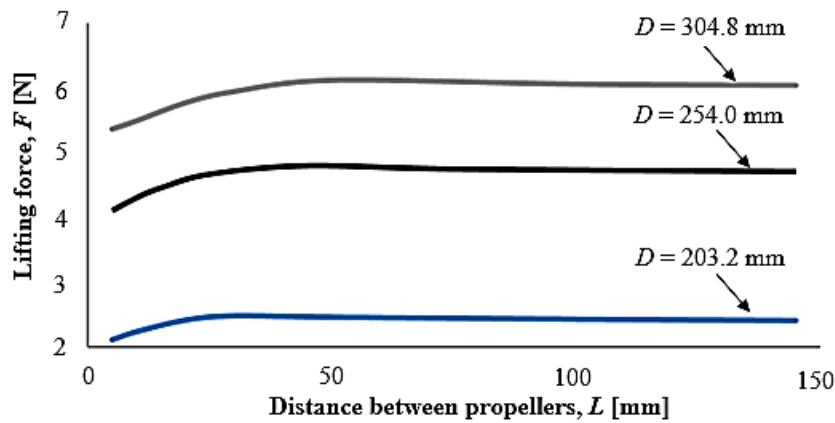


Figure 18. Lifting force produced by the propeller with the rotation speed of 5000 min^{-1} .

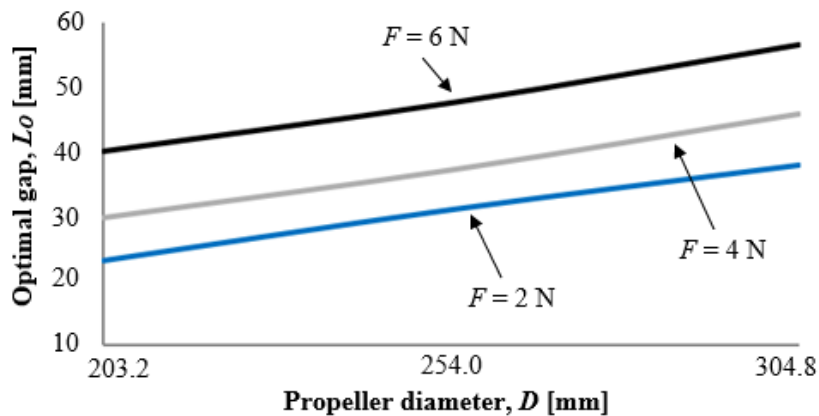


Figure 19. Optimal distances between propellers with different diameters (for generating force of 2 N, 4 N, and 6 N).

After substitutions in Eq. 5 and 6, Eq. 7 can be obtained. With this formula, it is possible to find an optimal distance between the propellers for a quadcopter with propeller pitch equal to half of the diameter at a defined lifting force. The calculation results are shown in Figure 20.

$$L = 0.55 \cdot F^2 - 0.24 \cdot F + 0.15 \cdot D - 8.35 \quad (7)$$

To ensure that Eq. 7 was applicable to a larger amount of propellers (not only for cases where the rotor’s pitch was equal to the radius), force correction should be added and the results can be presented as an equation pair (Eq. 8)

$$\begin{cases} F_c = \left(P - \frac{D}{2}\right) \cdot (3.27 \cdot 10^{-4} \cdot D - 4.72 \cdot 10^{-2}) \\ L = 0.55 \cdot (F + F_c)^2 - 0.24 \cdot (F + F_c) + 0.15 \cdot D - 8.35 \end{cases} \quad (8)$$

The coefficient of determination gave a very precise result. Changing the optimal distance by $\pm 8\%$, power consumption will change slightly, around 1%. Equation 8 can be used within the propeller’s diameter range 177.8 mm – 355.6 mm in which the pitch was equal to 0.3 – 0.7 of the propeller diameter. Propeller’s rotation speed must be within $2000 \text{ min}^{-1} - 8000 \text{ min}^{-1}$.

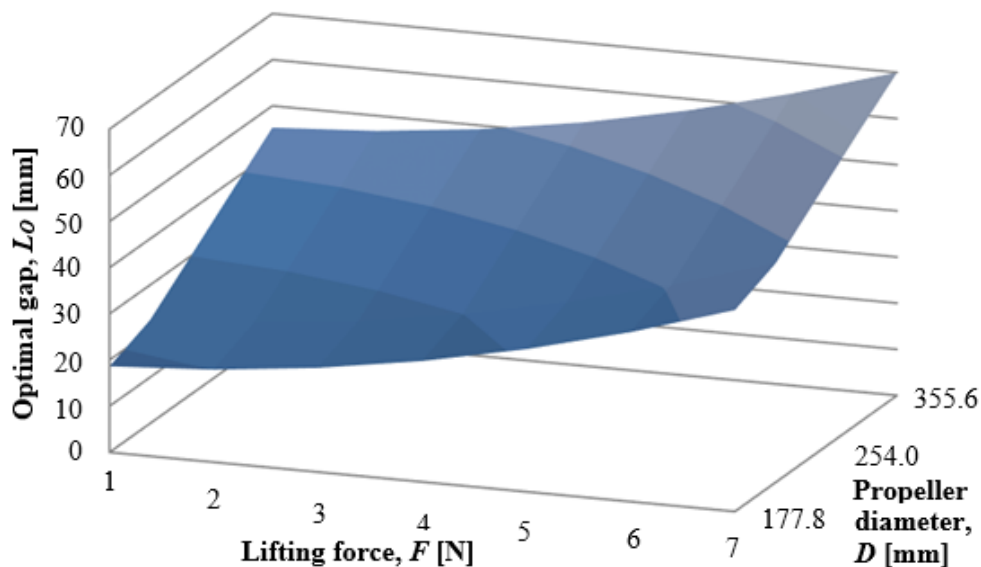


Figure 20. Optimal distances between the propellers.

To simplify the use of Eq. (8), widely used propeller sizes and masses of quadrotor helicopters were considered and the calculation results are presented in Table 1. The table contains optimal distances between propellers for different quadrotors, propeller pitches, and helicopter masses. Theoretically, the equation pair (Eq. 8) can be used not only for quadrotor helicopters but also for multicopters with 3, 6, 8, and other numbers of rotors.

Table 1. Optimal distance between axis of propellers, (mm).

Diameter [in]	Pitch [in]	UAV mass, [g]								
		1000	1250	1500	1750	2000	2250	2500	2750	3000
7	3.5	199	201	203	206	209	212	216	220	225
7	4.0	199	201	204	206	209	213	217	221	226
7	4.5	200	202	204	207	210	214	218	223	228
8	4.0	228	230	232	235	238	241	245	250	254
8	7.5	234	237	240	244	248	253	258	264	270
9	4.5	257	259	261	264	267	271	275	279	284
9	6.0	261	263	266	269	273	277	282	287	293
10	3.7	284	285	287	289	291	294	297	300	304
10	4.7	286	288	290	292	295	298	302	306	311
10	5.0	287	288	291	293	296	300	304	308	313
10	6.0	289	292	295	298	302	306	310	315	321
11	5.5	316	318	320	322	326	329	333	337	342
11	6.5	319	322	325	328	332	336	341	346	352
12	4.5	342	343	343	345	346	349	351	354	357
12	6.0	345	347	349	352	355	358	362	367	371
12	7.0	349	352	355	359	363	367	372	377	383
14	6.0	401	401	402	404	406	408	411	414	417
14	7.0	403	405	407	410	413	417	421	425	430
14	8.0	410	413	416	420	424	429	434	439	445

CONCLUSIONS

Lifting force of a quadcopter depends on different geometrical parameters. Normally, lifting force will increase with the increasing of propeller pitch. For different rotation velocities, this increasing is different but in all cases it can be approximated by a linear relationship. To obtain dependency functions, CFD simulations and laboratory experiments were carried out and an equation for calculation of lifting force, taking into account the pitch influence, was derived. Results showed a linear relationship between propeller pitch and the produced lifting force and proposed calculation equation gave reliable results at pitch values equal to 0.3 – 0.7 of the propeller diameter and at rotation velocities 2000 min^{-1} – 8000 min^{-1} . Analysis of mini quadcopter efficiency was carried out, taking into account the vehicle mass and lifting force produced by all propellers. CFD simulations showed that the lifting force of a quadcopter increased about 15% on the distances between propellers from 5 mm to 35 mm. From a distance of 70 mm, the lifting force will decrease about 2% and then will stabilise. Laboratory tests gave practically the same results. Deviation was about 3%. At increasing of distance between propellers from 5 mm until 25 mm, the power consumption decreased 8% - 10% and after the gap distance equal to 40 mm, it will be stable and minimal. Based on the experimental tests and analyses, one can assert that quadcopters have different optimal distances between the propellers at different rotation speeds to generate the same force. Equations for calculation of optimal gap distances for different multicopters were derived and calculation results were presented in graphs and tables. For example, for a quadcopter with propeller 254 mm x 127 mm and total mass of UAV equal to 1 kg, the optimal gap between propellers would be 33 mm. If the mass of the same design of UAV is equal to 2.5 kg, then the optimal gap would be 50mm.

ACKNOWLEDGEMENTS

This research work was supported by innovative Manufacturing Engineering Systems Competence Centre IMECC (supported by Enterprise Estonia and co-financed by the European Union Regional Development Fund, project EU48685); Estonian Research Council grant PUT1300; the Estonian Centre of Excellence in Zero Energy and Resource Efficient Smart Buildings and Districts, ZEBE, grant TK146 funded by the European Regional Development Fund.

REFERENCES

- [1] Coifman B, McCord M, Mishalani RG, Iswalt M, Ji Y. Roadway traffic monitoring from an unmanned aerial vehicle. *IEE Proceedings-Intelligent Transport Systems: IET*; 2006. p. 11-20.
- [2] Casbeer DW, Kingston DB, Beard RW, McLain TW. Cooperative forest fire surveillance using a team of small unmanned air vehicles. *International Journal of Systems Science*. 2006;37:351-60.
- [3] Xiaofeng L, Zhongren P, Zhang L, Li L. Unmanned aerial vehicle route planning for traffic information collection. *Journal of Transportation Systems Engineering and Information Technology*. 2012;12:91-7.
- [4] Jerry M. Current and Future UAV Military Users and Applications. *Air & Space Europe*. 1999;1:51-8.
- [5] Mejias L, Saripalli S, Campoy P, Sukhatme GS. Visual servoing of an autonomous helicopter in urban areas using feature tracking. *Journal of Field Robotics*. 2006;23:185-99.
- [6] Poyi GT, Wu MH, Bousbaine A, Wiggins B. Validation of a quad-rotor helicopter matlab/simulink and solidworks models. 2013.
- [7] Bousbaine A, Wu MH, Poyi GT. Modelling and simulation of a quad-rotor helicopter. 2012.
- [8] Wisniewski C, Byerley A, Van Treuren KW, Hays A. A Comparison of the Aerodynamic Performance and Aeroacoustic Behavior of Commercial and Custom Designed Quadcopter Propellers. *55th AIAA Aerospace Sciences Meeting 2017*. p. 1173.
- [9] Roldán JJ, Joossen G, Sanz D, del Cerro J, Barrientos A. Mini-UAV based sensory system for measuring environmental variables in greenhouses. *Sensors*. 2015;15:3334-50.
- [10] Xiang H, Tian L. Development of a low-cost agricultural remote sensing system based on an autonomous unmanned aerial vehicle (UAV). *Biosystems Engineering*. 2011;108:174-90.
- [11] Feng L, Ben MC, Yew LK. Integration and Implementation of a Low-cost and Vision-based UAV Tracking System. *Control Conference, 2007 CCC 2007 Chinese: IEEE*; 2007. p. 731-6.
- [12] Sharp CS, Shakernia O, Sastry SS. A vision system for landing an unmanned aerial vehicle. *Robotics and Automation, 2001 Proceedings 2001 ICRA IEEE International Conference on: Ieee*; 2001. p. 1720-7.
- [13] Girard AR, Howell AS, Hedrick JK. Border patrol and surveillance missions using multiple unmanned air vehicles. *Decision and Control, 2004 CDC 43rd IEEE Conference on: IEEE*; 2004. p. 620-5.

- [14] Peng K, Cai G, Chen BM, Dong M, Lum KY, Lee TH. Design and implementation of an autonomous flight control law for a UAV helicopter. *Automatica*. 2009;45:2333-8.
- [15] Walendziuk W, Oldziej D, Golinski P. A laboratory stand for research concerning drive units applied in unmanned flying micro vehicles. *Photonics Applications in Astronomy, Communications, Industry, and High-Energy Physics Experiments 2015: International Society for Optics and Photonics*; 2015. p. 966214.
- [16] Oldziej D, Gosiewski Z. Modelling of dynamic and control of six-rotor autonomous unmanned aerial vehicle. *Solid State Phenomena: Trans Tech Publ*; 2013. p. 220-5.
- [17] Hassanalian M, Abdelkefi A. Design, manufacturing, and flight testing of a fixed wing micro air vehicle with Zimmerman planform. *Meccanica*. 2017;52:1265-82.
- [18] KAMBUSHEV M, BILIDEROV S, VARBANOV Y. Synthesis And Study Of The Mathematical Model Of A Tricopter. *International Scientific Committee*. 2016:149.
- [19] Paw YC, Balas GJ. Development and application of an integrated framework for small UAV flight control development. *Mechatronics*. 2011;21:789-802.
- [20] Shim DH, Kim HJ, Sastry S. Control system design for rotorcraft-based unmanned aerial vehicles using time-domain system identification. *Control Applications, 2000 Proceedings of the 2000 IEEE International Conference on: IEEE*; 2000. p. 808-13.
- [21] Johnson EN, Kannan SK. Adaptive trajectory control for autonomous helicopters. *Journal of Guidance, Control, and Dynamics*. 2005;28:524-38.
- [22] Kambushev M. BS. Determination of aerodynamic coefficients necessary for the control of MAVs. *TransMotauto World*. 2017;2:94-7.
- [23] Yoon J, Lee J. Approximate Multi-Objective Optimization of a Quadcopter Through Proportional-Integral-Derivative Control. *Transactions of the Korean Society of Mechanical Engineers A*. 2015;39:673-9.
- [24] Sumantri B, Uchiyama N, Sano S. Least square based sliding mode control for a quad-rotor helicopter and energy saving by chattering reduction. *Mechanical Systems and Signal Processing*. 2016;66:769-84.
- [25] Kendoul F. Survey of advances in guidance, navigation, and control of unmanned rotorcraft systems. *Journal of Field Robotics*. 2012;29:315-78.
- [26] Zhang W, Fan N, Wang Z, Wu Y. Modeling and aerodynamic analysis of a ducted-fan micro aerial vehicle. *Modelling, Identification & Control (ICMIC), 2012 Proceedings of International Conference on: IEEE*; 2012. p. 768-73.
- [27] E. JN. *Theory of Elasticity, Railways, Automobiles. Collected Papers*. 1937;III:48-56.
- [28] Velikanov N, Koryagin S, Sharkov O. Definition of Locked-up Stresses around a Rectilinear Welding Seam. *IOP Conference Series: Materials Science and Engineering: IOP Publishing*; 2016. p. 012094.
- [29] Sharkov O, Kalinin A. Kinematic characteristics of pulsed speed regulators. *Russian Engineering Research*. 2009;29:551-4.
- [30] Eleftherios A, Tsili MA, Spathopoulos V, Hatziefremidis A. Energy Efficiency Optimization in UAVs. *Materials Science Forum 2014*. p. 281-6.
- [31] Wisniewski CF, Byerley AR, Heiser W, Van Treuren KW, Liller T. Designing Small Propellers for Optimum Efficiency and Low Noise Footprint. *33rd AIAA Applied Aerodynamics conference 2015*. p. 2267.

- [32] Wisniewski CF, Byerley AR, Heiser W, Van Treuren KW, Liller T. The Influence of Airfoil Shape, Reynolds Number and Chord Length on Small Propeller Performance and Noise. 33rd AIAA Applied Aerodynamics Conference 2015. p. 2266.
- [33] Ramasamy D, Yuan GC, Bakar RA, Zainal Z. Validation Of Road Load Characteristic Of A Sub-Compact Vehicle By Engine Operation. International Journal of Automotive & Mechanical Engineering. 2014;9.
- [34] Otsuka H, Nagatani K. Thrust loss saving design of overlapping rotor arrangement on small multirotor unmanned aerial vehicles. Robotics and Automation (ICRA), 2016 IEEE International Conference on: IEEE; 2016. p. 3242-8.
- [35] Aleksandrov D, Penkov I. Optimization of Lift Force of Mini Quadrotor Helicopter by Changing of Gap Size Between Rotors. Solid State Phenomena: Trans Tech Publ; 2013. p. 226-31.
- [36] Sakinah MH, Amirruddin AK, Kadirgama K, Ramasamy D, Rahman MM, Noor MM. The application of response surface methodology in the investigation of the tribological behavior of palm cooking oil blended in engine oil. Advances in Tribology. 2016;2016.
- [37] Najiha M, Rahman M, Kadirgama K, Noor M, Ramasamy D. Multi-objective optimization of minimum quantity lubrication in end milling of aluminum alloy AA6061T6. International Journal of Automotive and Mechanical Engineering. 2015;12:3003.

NOMENCLATURE

- UAV – Unmanned Aerial Vehicle,
- CFD – Computational Fluid Dynamics,
- FVM – Finite Volume Method,
- D – propeller diameter, N,
- F – lifting force, N,
- F_1 – required one propeller lifting force for holding helicopter in hover, N,
- F_C – overall coefficient of the correction of lifting force, N,
- F_{C-8} – correction coefficient of lifting force for 203.2 mm propeller, N,
- F_{C-10} – correction coefficient of lifting force for 254 mm propeller, N,
- F_{C-12} – correction coefficient of lifting force for 304.8 mm propeller, N,
- L – gap distance between propellers, mm,
- L_O – optimal gap distance between propellers, mm,
- L_{O-10} – optimal gap distance between 254 mm propellers, mm,
- L_d – optimal gap distance on the propeller diameter, mm,
- N – power, W,
- P – propeller pitch, mm,
- R – propeller radius, mm,
- n – rotation speed, min^{-1} ,
- α – angle between the propeller cord and the horizontal plane, deg.